

ANALYSIS OF A SUBSIDENCE PROCESS BY INTEGRATING GEOLOGICAL AND HYDROGEOLOGICAL MODELING WITH SATELLITE INSAR DATA

Bozzano F.^(1,2), Esposito C.⁽¹⁾, Franchi S.⁽¹⁾, Mazzanti P.^(1,2), Perissin D.⁽³⁾, Rocca A.⁽¹⁾, Romano E.⁽⁴⁾

⁽¹⁾ *Department of Earth Sciences – Sapienza, University of Rome, P.le Aldo Moro, 5 Rome, Italy, francesca.bozzano@uniroma1.it; carlo.esposito@uniroma1.it; franchistefania@libero.it; alfredo.rocca@uniroma1.it*

⁽²⁾ *NHAZCA S.r.l. - Spin off of Sapienza, University of Rome, Via Cori, Rome, Italy, paolo.mazzanti@nhazca.com*

⁽³⁾ *Institute of Space and Earth Information Science – Chinese University of Hong Kong, Fok Ying Tung Remote Sensing Science Building, The Chinese University of Hong Kong, Shatin, Hong Kong, daniele.perissin@cuhk.edu.hk*

⁽⁴⁾ *Water Research Institute – National Research Council, Via Salaria 29,300 -00015 Monterotondo Scalo (Rome), Italy, romano@irsa.cnr.it*

ABSTRACT

This paper focuses on a multidisciplinary study carried out in an urban area affected by subsidence and related structural damages. The study area is located about 20 km east of Rome (Italy) and is characterized by a relevant groundwater exploitation for various purposes as well as by the presence of compressible soils immediately below the ground level. Extensive processing at different scales of SAR satellite images (ERS and ENVISAT provided by ESA in the frame of a CAT-1 proposal) by means of PSInSAR technique was performed. The so reconstructed time histories of ground displacements were then coupled and compared with a detailed geological model and the variations over time of piezometric levels, obtained by means of a 3D numerical model of groundwater circulation. Such a data overlay over time and space allowed us to better understand and constrain the relationships among ground displacement, piezometric variations, geological setting and geotechnical properties of subsoil.

1. INTRODUCTION

The Acque Albule basin is a quite flat area located about 20 km east of Rome which is affected by a relevant subsidence process, as visible in Fig. 1 and clearly testified by significant damages to several buildings related to differential settlements (Fig. 2). In terms of structural damages, the subsidence process started to involve buildings in the mid 80's of last century and increased at the beginning of 2000's, even causing the evacuation of some houses and public buildings. In the first instance, it is possible to state that several potential predisposing/triggering factors for the observed subsidence are present in the study area: i) the presence of compressible soils in the first meters of the local substratum; ii) a continuously growing urbanization (with related overloads); iii) a very significant groundwater exploitation (and related water table lowering) due to the presence of a variety of "anthropic stresses", i.e. quarry activities and several agricultural and domestic wells. The here presented study aims at defining the recent "time history" of ground deformations by means of advanced DInSAR techniques, to be compared with the piezometric variations (both measured and simulated by means of numerical modeling) and the stratigraphic setting (obtained by interpolating data from several available and on-purpose drilled boreholes), in order to better understand and constrain the relationships among subsidence (in terms of both magnitude and rate), timing of piezometric level variations and thickness of compressible soils. It is worth noting that the here

presented methodologies and results at the basin scale are framed within a research project (PRIN 2010) funded by Italian Ministry of Education, University and Research (MIUR): within this project an experimental site has been equipped with multi-base electric piezometers and an assestimeter for a very detailed analysis of the cause-effect relationships among subsidence rate, pore water pressure variations and stratigraphical/geotechnical setting of subsoil.

2. GEOLOGICAL AND HYDROGEOLOGICAL BACKGROUND

The Acque Albule Basin is a morphotectonic depression, whose formation and development is related to the Plio-Quaternary activity of strike-slip tectonic elements (Fig. 3). The so formed depression, whose bedrock is featured by meso-cenozoic limestone, hosted the deposition of Plio-Pleistocene alluvial, lacustrine, and epivolcanic deposits. These deposits are in turn covered by a thick (up to 80 m) travertine cover, well known since the Ancient Roman age with the name of Lapis Tiburtinus. Such a travertine cover is mainly made up of stiff and cemented calcite, whose precipitation and growth occurred in several phases between 115- 30 ka [1], [2], [3] and is strictly connected with the deep hydrothermal circulation into the Meso-Cenozoic limestone. Moving upward within the stratigraphic sequence, the travertine plateau is overlaid by a discontinuous cover of a weakly cemented up to loose travertine, composed by clasts interspersed in a sandy-silty matrix



Legend
PS
Vel LOS (mm/year)

- < -25.00
- -24.99 - -10.00
- -9.99 - -5.00
- -4.99 - -3.00
- -2.99 - -1.50
- -1.49 - 1.50
- 1.51 - 3.00
- 3.01 - 5.00
- 5.01 - 10.00
- 10.01 - 25.00
- >25.00

- Quarries
- Aniene river

0 1 km

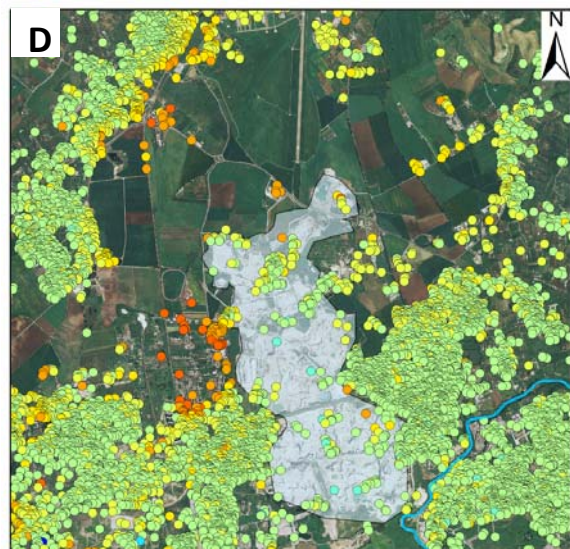
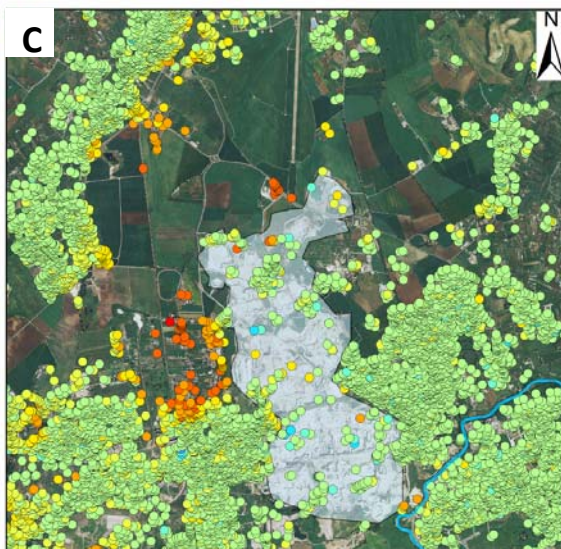
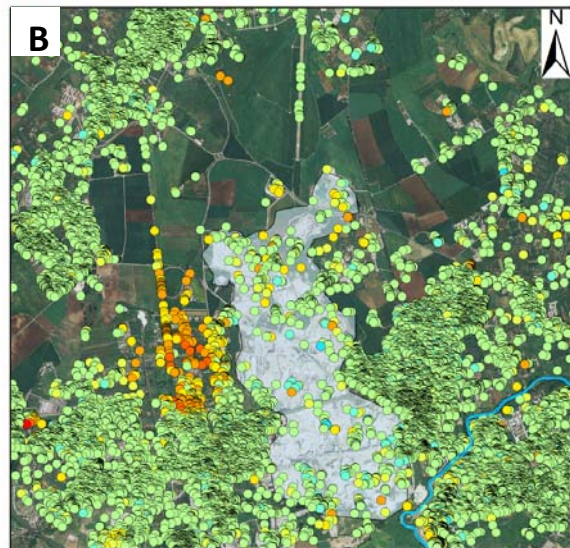
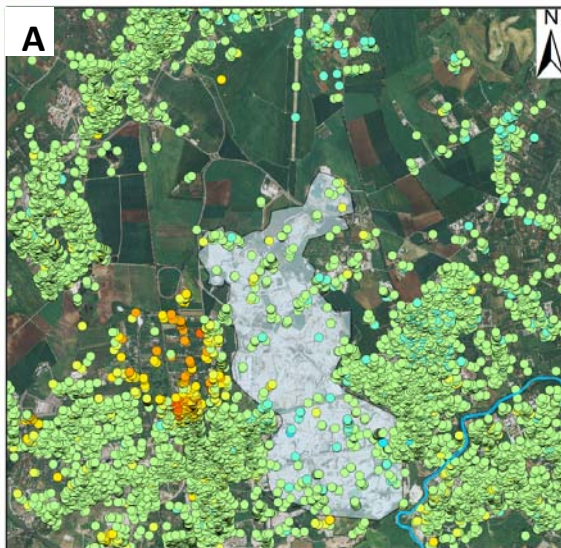


Figure 1. Maps of the mean annual subsidence rate along Line of Sight, (LOS) obtained by processing satellite images from ERS ascending (A), ERS descending (B), ENVISAT ascending (C) and ENVISAT descending (D).

Finally, the development of karst collapses within the travertine caused the formation of morphological depressions which hosted a lacustrine-palustrine environment with the deposition of sandy silts, clay-loam (with high organic content) and peats.

The last two geological units (namely, loose travertine sandy silts and organic clay-loam and peat), that in a first instance can be grouped in a “compressible” geological-technical unit, have a quite variable thickness below the ground level, ranging between few centimeters up to more than 10 meters, as revealed by the geological model interpolated on the basis of available stratigraphic logs (Fig. 4).



Figure 2. Effects on buildings induced by subsidence: examples of structural (left) and non-structural (right) damages.

Strictly related to the quite complex geological setting is the multi-level groundwater circulation in the Acque Albule Basin (Fig. 3). The Meso-Cenozoic limestone hosts a deep aquifer fed laterally by the deepest part of the surrounding carbonate ridges, outcropping east and

north-east of the basin. The waters contained herein is thermalized due to the rise of deep fluids at high pressure and temperature from the supply system of the Colli Albani volcanic complex, which outcrops southward. The aquifer is confined at the top by clayey-sandy deposits that act as aquitard / aquiclude thus providing a piezometric level even higher than the ground level. The aquitard separates the deep aquifer from the most superficial hosted in the travertine plateau and fed by contributions directly from rainfall and laterally by the above mentioned surrounding carbonate ridges. In addition, such an aquifer is partially fed by the upwelling of thermalized waters (and gas), coming from the deep aquifer and passing through the tectonic discontinuities which drove the formation of the basin itself [3], [4], [5], [6], [7]. Several springs with significant discharge testify for the huge potential of such an aquifer.

Notwithstanding, the “superficial” aquifer is stressed by human activities so much that the water balance is unstable: a generalized lowering of the water table affects a wide portion of the Acque Albule Basin, while a more significant dewatering (and related piezometric level lowering) involves the areas surrounding the travertine quarries where water pumping (on the order of 4 m³/s) is necessary to exploit deep travertine banks. Such a quarrying activity increased in the last decades, thus causing a progressive enlargement and deepening of the related cone of depression. Based on the collection of hydrogeological monitoring data as well as on hydrodynamic parameters, a detailed hydrogeological 3D numerical model was performed [8] by updating and refining a previous one [9]. Such a model allowed us to reconstruct with a good degree of confidence the “time history” of the dewatering process over time and space (Figs. 5 and 6).

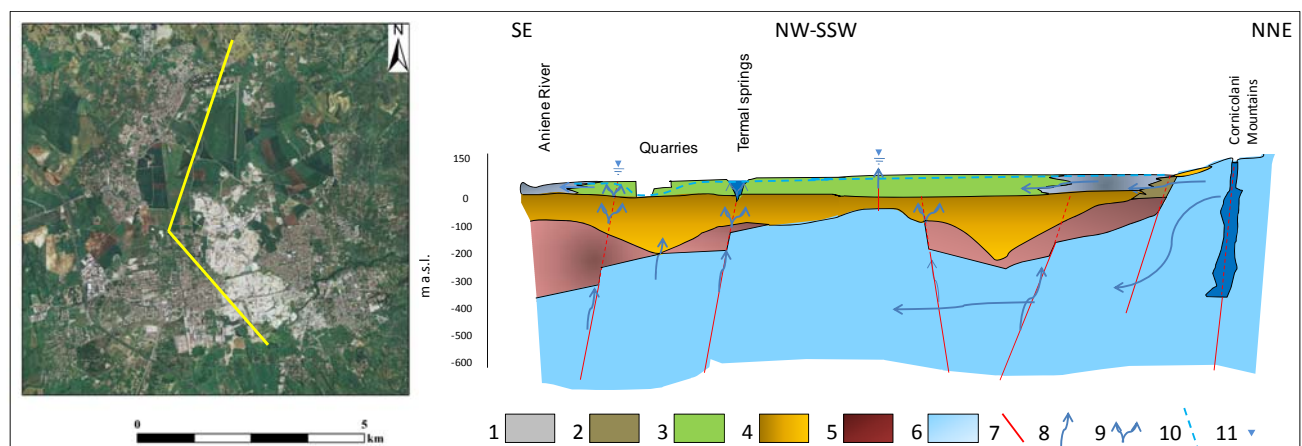


Figure 3. Simplified geological and hydrogeological cross-section of the Acque Albule Basin. Key to legend: 1) recent alluvial and colluvial deposits; 2) Debris; 3) Travertine and lacustrine/palustrine deposits; 4) Pleistocene deposits; 5) Pliocene deposits; 6) Carbonatic bedrock; 7) Fault; 8) Flow direction; 9) Groundwater overspill; 10) Water table level; 11) Confined water table level. Modified after [7].

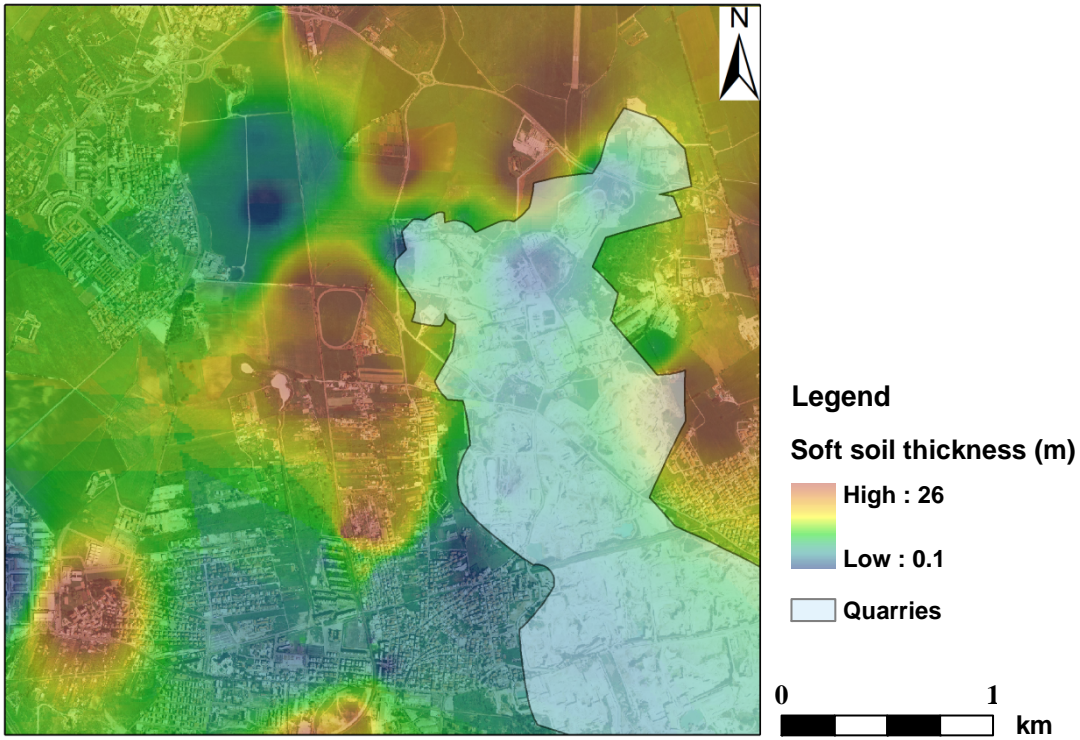


Figure 4. Map representing the spatial distribution of soft soil thickness.

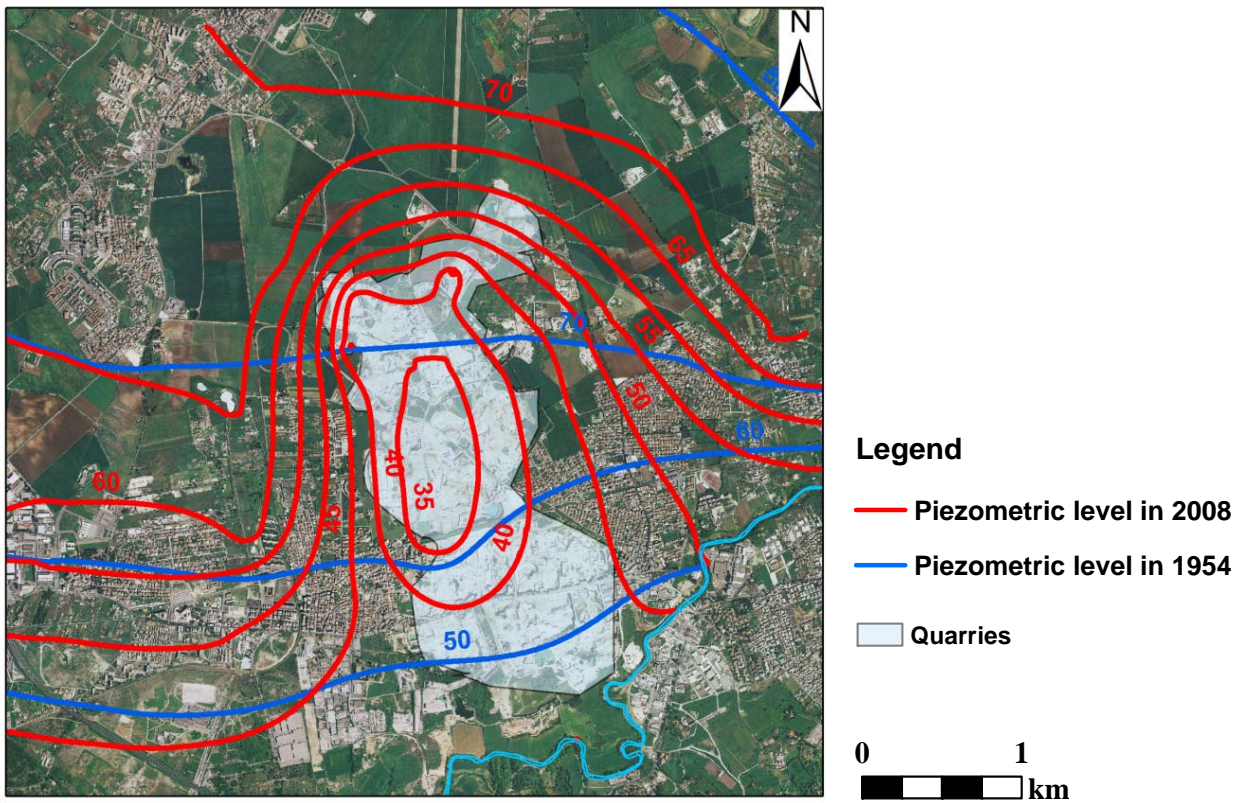


Figure 5. Reconstruction via numerical modelling of piezometric levels within travertine in undisturbed (1954) and disturbed (2008) conditions.

3. INTERFEROMETRIC ANALYSES

The above depicted geological and hydrogeological frame is robust enough to more deeply understand the relative weight of different factors in the activation of subsidence, once the “time history” of ground deformation is reconstructed by means of SAR data.

In this work, ground subsidence measurements were

obtained using PSInSAR technique [10], [11], [12], [13], [14] and using proprietary procedures implemented in SARPROZ software (Copyright (c) 2009 Daniele Perissin, Italy) [15], [16], [17], which uses genetic algorithms to calculate parameters derived from processing of interferometric data.

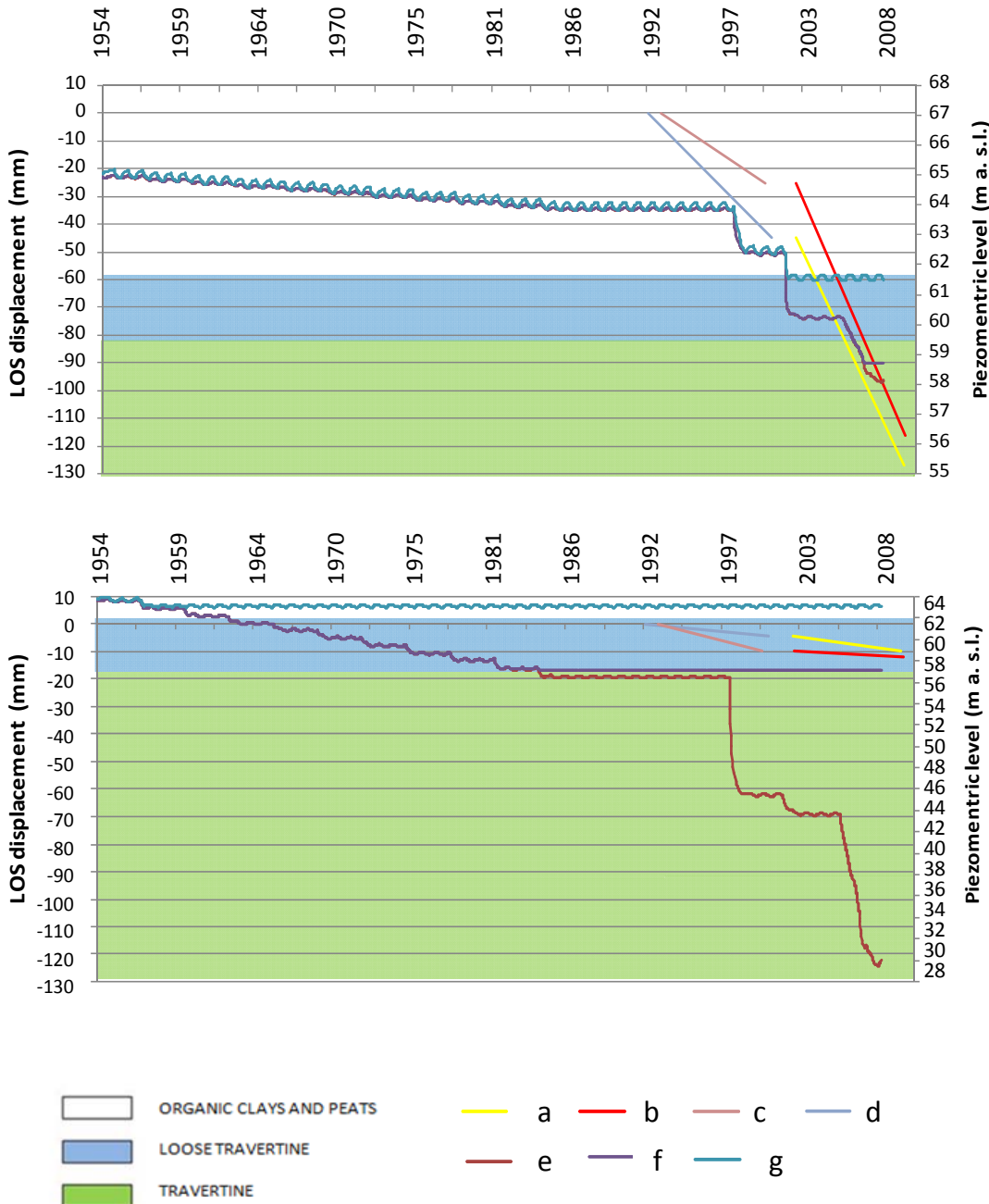


Figure 6. Charts showing the relationships between the time histories of modelled dewatering and LOS displacement in two different stratigraphic settings. Key to legend: a) ENVISAT descending; b) ENVISAT ascending; c) ERS ascending; d) ERS descending; e) Simulated piezometric level in travertine; f) Simulated piezometric level in loose travertine; g) Simulated piezometric level in organic clays and peats.

The analysis was carried out through two main approaches: full-site processing and local scale processing. Full-site processing allowed us to reconstruct the deformational trend of the entire basin, with the aim of characterizing a large portion of territory in terms of mean annual Line of Sight (LOS) velocity. Additional analyses were performed on a local scale and focused on areas of greatest interest, in order to identify possible non-linear trends correlated with piezometric level variations caused by human activity. ERS and ENVISAT data stacks, provided by ESA in the frame of the CAT-1 project “Geological reconstruction and monitoring in recently urbanized areas affected by subsidence” (ID: 13097), both in ascending and descending acquisition geometry, were processed independently and combined only as final geocoded products in a GIS system: use was made of 192 Synthetic Aperture Radar (SAR) scenes, covering the period June 1993–August 2010. For each path and

frame we selected a single master and co-registered all slave images to that master.

With regard to full-site analyses, PS candidates (PSC) were selected based on a combination of several quality parameters related to the amplitude of the radar signal (reflectivity and Amplitude Stability Index – ASI). A network of PSC was created to estimate preliminary height and velocity parameters, in order to retrieve and remove the Atmospheric Phase Screen (APS). After APS removal, a second parameters estimation was performed on a wider set of points, selected on a spatial coherence and ASI combination criterion. For the displacement parameter, a linear deformation trend model was adopted. At the end of the PS analyses, all PSs with coherence above 0.65 were selected. For each PS, LOS velocity, displacement time series and height were computed (related to a reference point identified in a stable area outside the Acque Albule Basin).

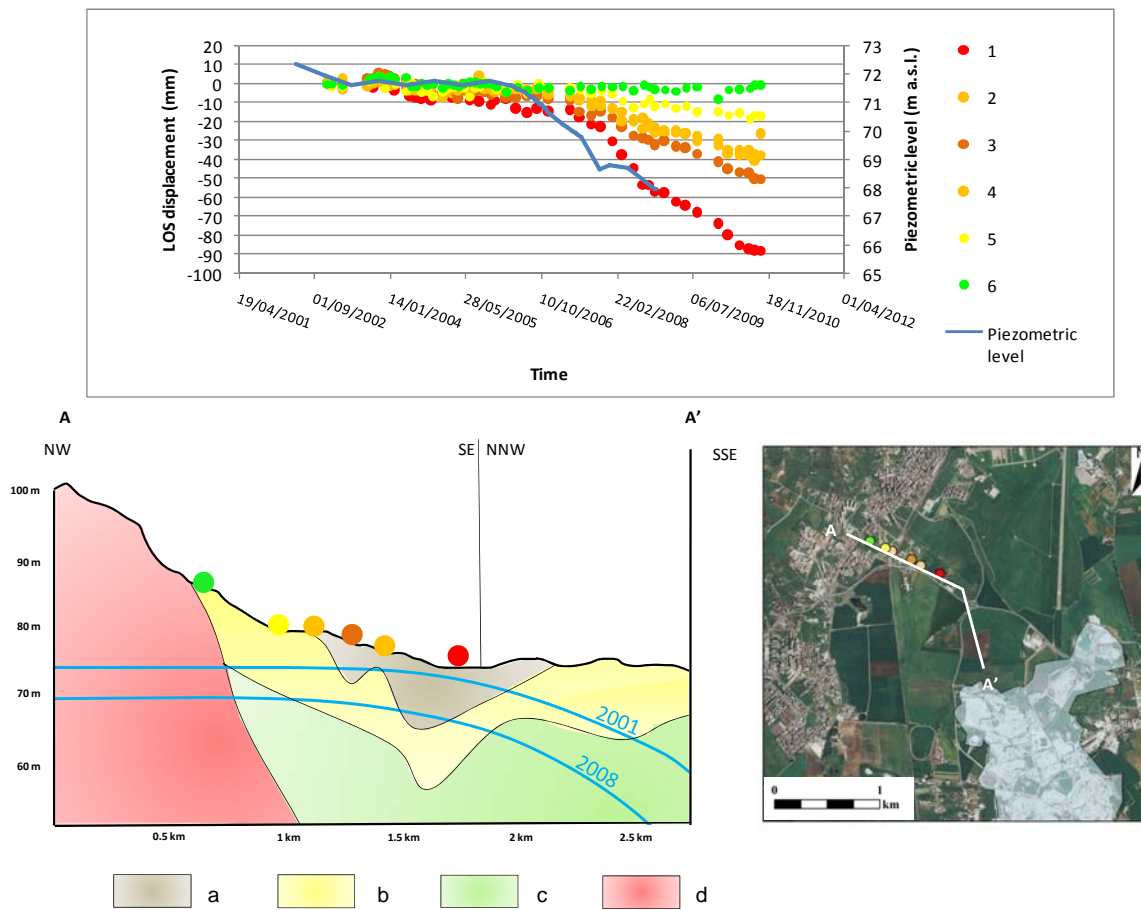


Figure 7. Chart showing the relationships between the time histories of modelled dewatering and LOS displacement of selected PSs along a transect at the NW border of the basin. The stratigraphy associated to the selected PSs as well as their location are reported in the lower left and lower right corners, respectively. Key to legend: a) Organic clays and peats; b) Loose travertine; c) Travertine; d) Volcanic deposits.

The analysis at locale scale, carried out to highlight non-linear and/or cyclical deformation, was performed on

the portion of the basin that was progressively involved in the dewatering. Eight sectors (with an area smaller

than 2 km²) of the basin were analyzed separately. This approach does not require the estimation and removal of APS because atmospheric perturbations have a correlation distance less than 1 km [18]. In contrast, non-linear movements are expected to show smaller correlation in space; thus, we assumed to be able to detect such movements via a low pass filter in time domain. The choice of the reference point for each area was performed selecting it in stable areas outside of the basin. PSC were then chosen by applying a threshold value on ASI. For the selected points, height and displacement were estimated and deformation time series were reconstructed.

4. RESULTS AND CONCLUDING REMARKS

In first instance, by overlaying a classified post map of the full-site PS analysis and the map representing the distribution of compressible soil thickness, it is possible to observe in general terms the relationship among subsidence average rate and geological setting. Furthermore, if the “time history” of some selected PS is compared to the modeled piezometric level variations over time, an acceleration of the subsidence process can be pointed out in correspondence of the main dewatering phases (fig. 6), thus confirming the relevant role of water pumping. When water is pumped from the travertine aquifer, whose piezometric level roughly coincided with the ground level in undisturbed conditions, a gradient is created thus implying a water flow from the topmost compressive soils down to the travertine aquifer. As a result, pore pressure decreases and the soil experiences a consolidation process. At the same time, figure 6 shows the different behaviour of the PSs as a function of the local stratigraphy, being comparable the dewatering magnitude.

More detailed hints derive from the local scale analysis: in this paper we show the results from an area located at the NW border of the basin, which is particularly significant as: i) it encompasses a variety of stratigraphic settings; ii) it has been involved in the cone of depression recently, so that significant piezometric variations can be noted in the investigated time interval (2001-2010). Figure 7 clearly shows that the activation time of subsidence is strictly related to the involvement in the cone of depression, while the magnitude of the process is governed by the local stratigraphy. This evidence is testified by the behaviour of some PSs farther away from the pumping “epicenter” that experience greater vertical movements than other points located closer: the associated stratigraphy reveals a thicker layer of compressible soils in the former points with respect to the latter ones. Finally, as expected, PSs located on the outcropping volcanic units are not affected by significant vertical deformations.

The here presented results are encouraging for the final goal of the research project in whose frame these activities were carried out: the project focuses on the

back-analysis of factors which control onset and development of subsidence, with the final aim of attempting to forecast subsidence activation and magnitude on the basis of piezometric monitoring coupled with a detailed knowledge of the geological-technical model of the subsoil. In this sense, a contribution could derive from the aforementioned hydrogeological/geotechnical experimental test site aimed at better quantifying the relationships among water level/pressure variations, geological setting and geotechnical properties.

5. REFERENCES

1. Faccenna, C., Funicello, R., Mattei, M. (1994). Late Pleistocene N-S shear zones along the Latium Tyrrhenian margin: structural characters and volcanological implications. *Bol. Geofis. Teorica Appl.* **36**, 507-522.
2. Billi, A., Valle, A., Brilli, M., Faccenna, C., Funicello, R. (2007). Fracture-controlled fluid circulation and dissolutional weathering in sinkhole-prone carbonate rocks from central Italy. *J. Struct. Geol.* **29**, 385–395.
3. Faccenna, C., Soligo, M., Billi, A., De Filippis, L., Funicello, R., Rossetti, C., Tuccimei, P. (2008). Late Pleistocene cycles of travertine deposition and erosion, Tivoli, Central Italy: possible influence of climate changes and fault-related deformation. *Global Planet. Change.* **63**(4), 299–308.
4. Boni, C., Bono, P., Capelli, G. (1986). Schema idrogeologico dell'Italia Centrale [Hydrogeological scheme of Central Italy]. *Mem. Soc. Geol. It.* **35**, 991–1012.
5. Capelli G., Cosentino D., Messina P., Raffi R., Ventura G. (1987). Modalità di ricarica e assetto strutturale dell'acquifero delle sorgenti Capore - S. Angelo (Monti Lucretili - Sabina Meridionale). *Geologica Romana.* **26**, 419–447.
6. Faccenna C. (1994). Structural and hydrogeological features of Pleistocene shear zones in the area of Rome (central Italy). *Annali di Geofisica.* **37**(1), 121-133.
7. Capelli, G., Mazza, R., Taviani, S. (2005). Studi idrogeologici per la definizione degli strumenti operativi del piano stralcio per l'uso compatibile delle risorse idriche sotterranee nell'ambito dei sistemi acquiferi prospicienti i territori vulcanici laziali. Relazione inedita, Università degli Studi di Roma III, dipartimento di Scienze Geologiche, Laboratorio di Idrogeologia.
8. Franchi S. (2012). Effetti del depauperamento dell'acquifero principale della piana di Tivoli-

Guidonia sulla compattazione dei sedimenti recenti. Tesi di laurea, Università La Sapienza, Roma.

9. Brunetti, E., Jones, J.P. & Petitta, M. (2013). Assessing the impact of large-scale dewatering on fault-controlled aquifer systems: a case study in the Acque Albule basin (Tivoli, central Italy). *Hydrogeology Journal*, **21**, 401-423.
10. Ferretti A., Prati C. & Rocca F. (2000). Non-linear subsidence rate estimation using permanent scatterers in differential SAR interferometry. *IEEE Trans. Geosci. Remote Sensing*. **38**, 2202–2212.
11. Ferretti A., Prati C. & Rocca F. (2001). Permanent scatterers in SAR interferometry. *IEEE Trans. Geosc. and Remote Sens.* **39**(1), 8-20.
12. Kampes, B. (2006). *Radar Interferometry: Persistent Scatterer Technique*. Dordrecht. Springer-Verlag.
13. Hooper, A., Zebker, H., Segall, P., Kampes, B. (2004). A new method for measuring deformation on volcanoes and other natural terrains using InSAR Persistent Scatterers. *Geophys. Res. Lett.* **31**. doi:10.1029/2004GL021737.21.
14. Berardino, P., G. Fornaro, R. Lanari, and E. Sansosti (2002). A new algorithm for surface deformation monitoring based on small baseline differential SAR interferograms. *IEEE Trans. Geosci. Remote Sensing*. **40**, 2375 – 2383.
15. Perissin D., (2009). SARPROZ Manual http://ihome.cuhk.edu.hk/~b122066/index_files/download.htm.
16. Perissin D., Wang Z. & Wang T. (2011). The SARPROZ InSAR tool for urban subsidence/manmade structure stability monitoring in China. Proc. of ISRSE 2010, Sidney, Australia, 10-15 April 2011.
17. Perissin D. & Wang T. (2012). Repeat-Pass SAR Interferometry With Partially Coherent Targets. *IEEE Trans. on Geosc. and Remote Sens.* **50**(1), 271, 280.
18. Hanssen, R. (2001). *Radar interferometry, data interpretation and error analysis*. Kluwer Academic Publishers.